Efficient extraction of multivalent cations from aqueous solutions into sitinakite-based sorbents

Perovskiy, Igor A.; Khramenkova, Elena V.; Pidko, Evgeny A.; Krivoshapkin, Pavel V.; Vinogradov, Alexandr V.; Krivoshapkina, Elena F.

DOI
10.1016/j.cej.2018.08.030

Publication date
2018

Document Version
Accepted author manuscript

Published in
Chemical Engineering Journal

Efficient extraction of multivalent cations from aqueous solutions into Sitinakite-based sorbents

Igor A. Perovskiy[1], *Elena V. Khramenkova*[2], *Evgeny A. Pidko*[2,3], *Pavel V. Krivoshapkin*[2], *Alexandr V. Vinogradov*[2], *Elena F. Krivoshapkina*[2,4]

[1]Institute of Geology, Komi Science Center, Ural Branch of the Russian Academy of Sciences, Syktyvkar, 167982, Russian Federation

[2]ITMO University, Saint Petersburg, 197101, Russian Federation

[3]Inorganic Systems Engineering group, Department of Chemical Engineering, Faculty of Applied Sciences, Delft University of Technology, 2629 HZ Delft, The Netherlands

[4]Institute of Chemistry, Komi Science Center, Ural Branch of the Russian Academy of Sciences, Syktyvkar, 167982, Russian Federation

Corresponding author: Krivoshapkina E.F.

e-mail: chemicalfox@mail.ru

Abstract

A highly selective adsorbent for multivalent cationic species based on a sitinakite-type titanosilicate was prepared from a leucoxene ore enrichment waste. The synthesized material was used as for the selective removal of alkali-earth strontium (II) and barium (II) cations as well as for the cationic species based on the natural isotopes of uranium, radium, and thorium from aqueous solutions. The influence of such parameters as the pH, the initial concentration of the ions, the presence of other electrolytes on the sorption parameters was investigated. The sorption capacity of the synthesized material at ambient conditions is 80 and 110 mg/g for Sr^{2+} and Ba^{2+}, respectively, and it rises with increasing temperature. Furthermore, the material shows a high selectivity towards radionuclides of radium, uranium, and thorium. By using the current titanosilicate materials, the extracting degree of over 99% could be achieved when extracting these species from their respective standard aqueous solutions. The origin of the high adsorption selectivity for cationic complexes of thorium and uranium is rationalized based on periodic density functional theory calculations. The obtained results indicate that the described materials could be promising and inexpensive sorbents for the selective extraction of radioactive isotopes and particularly those of Sr, Ba and U, Th, Ra.

Keywords

Titanosilicate, Sitinakite, Leucoxene ore, Hydrothermal synthesis, Sorption, Radionuclides, Radioactive waste

1. Introduction

Accumulation of radioactive waste at nuclear power plants is an important problem of our civilization leading to catastrophes on a regional and global level. Due to diversity of the sources of origin, radioactive waste has a wide variety of compositions and physicochemical properties. The greatest danger to the biosphere is posed by liquid radioactive waste containing radionuclides of ^{137}Cs and ^{90}Sr with high heat release rate, often in combination with long-lived ($T_{1/2}>10^5$ years) α-emitting actinides. Selective removal of ionic forms of these radionuclides from aqueous media is a challenge that can be tackled using a number of approaches such as the extraction, anion and cation exchange, phytoremediation and vacuum evaporation [1-4]. Among these processes particularly interesting and attractive are the sorption methods employing inorganic ion-exchange materials showing high selectivity, chemical stability, thermal and radiation resistance. The most studied inorganic sorbents are metal oxides, graphene oxides, inorganic salts, modified or synthetic clays, natural and synthetic zeolites (mostly NaX and NaA zeolites), and porous titanosilicates [5-16].

Synthetic analogs of titanosilicate natural minerals, whose variety is associated with alkaline complexes of the Kola Peninsula, have recently attracted increased attention. Among natural titanosilicates the zorite, sitinakite, lintisite, and ivanyukite minerals are widely known as prototypes of the synthetic materials ETS-4, CST (IONSIV IE-910, IONSIV IE-911), AM-4 and ivanyukite-Na(K) [17-20]. These materials have found application in the selective extraction of radionuclides (Cs, Sr, U, Pu, Am) from weakly acidic, neutral and alkaline solutions [21-30]. An important factor in using titanosilicates in sorption processes for extracting radionuclides is the possibility of obtaining mineral-like SYNROC (SYNtheticROCk) ceramics as produced by Ringwood at the Australian National University at temperatures below 1000°C [31-33]. Such

ceramics are resistant to leaching as well as to various mechanical, thermal, and biological effects. They usually have a high waste loading capacity, show a substantial radiation resistance. Synthetic titanosilicates (CST, ETS-10) saturated with waste components (UO_2^{2+}, Cs^+, and Sr^{2+}) undergo thermal transformations into a consolidated glass crystalline form, in which uranium is evenly distributed in the titanosilicate matrix without the formation of intrinsic phases [30], cesium cations are included in the $CsTiSi_2O_{6.5}$ phase analogous to pollucite [34-36] and strontium cations are in the $Sr_2TiSi_2O_8$ phase similar to fresnoite [18, 37].

Synthesis of titanosilicates is typically carried out under mild hydrothermal conditions using such titanium sources as titanium isopropyloxide $Ti(OC_3H_7)_4$, titanium dioxide TiO_2, sodium peroxotitanate Na_4TiO_6 obtained from $Ti(OC_3H_7)_4$ or $TiOCl_2$, as well as $TiCl_4$. Common silicon sources are the colloidal silicon (Ludox-AS-40, Ludox-HS-40), pyrogenic silicon dioxide, silica gel, silicon dioxide with various particle sizes (12 to 200 μm) or tetraethyl orthosilicate $(C_2H_5O)_4Si$ [38-46]. All these synthesis methods involve the use of expensive reagents, which strongly hinders the utilization of the resulting materials as the adsorbents. One of the most urgent tasks for the introduction of titanosilicates into the industry is the search of alternative precursors for their synthesis.

Synthetic methods utilizing various abundant sources of silicon have already been described. For example, Ismail and co-authors [47] used sea white sand as the silicon source, Liying Liu and co- authors [48] proposed to utilize ashes of power stations, and Yew-Choo and authors [49] described a synthesis methodology based on the ashes of rice husk. Nevertheless, the main costs of producing titanosilicate compounds are not related to silica, but to the titanium component. The high cost of titanium-containing precursors necessitates the search for new components for synthesis, which can be represented by inexpensive natural raw materials, such as leucoxene

(titanium) ores of the Yaregskoye deposit of the Komi Republic, Russia. In this paper, we have combined a variety of experimental and theoretical approaches to determine the potential of such feedstock for the synthesis of sitinakite-type sorption materials and investigate its sorption characteristics for extracting common radionuclides from aqueous solutions.

2. Materials and methods

2.1. Materials

NaOH (purity ≥98%, Fluka), $SrCO_3$ (≥ 98%, Aldrich), $BaCl_2 \cdot 2H_2O$ (> 99%, Sigma-Aldrich), NaCl (>99,5 %, Fluka), NH_4Cl (99,99 %, Aldrich), HCl (puriss. spec., Sigma Tec), NH_4OH (puriss. spec., Sigma Tec) were used as received without additional purification. For the preparation of working solutions, deionized water with a specific resistance of 10 Mohm·cm was used. The hydrated precipitate used for the synthesis of titanosilicate was prepared with the original fluorammonium method of processing leucoxene concentrate of the Yaregskoye deposit [50]. The chemical composition of the hydrated precipitate was determined using X-ray fluorescence analysis and presented in Table S1.

2.2. Synthesis of sitinakite

Sitinakite was synthesized using the traditional hydrothermal method. The dried hydrated precipitate, 0.5 g, was treated with 37 mL of 1M NaOH solution and dispersed for 20 minutes with a magnetic stirrer. The reaction suspension with a molar composition of $1TiO_2 – 1.2SiO_2 – 5.98Na_2O – 657.7\ H_2O$ was placed in 45 mL autoclave with a Teflon liner, and the hydrothermal reaction was carried out at 250°C for 12 hours. After having cooled down naturally to room

temperature, the product was collected by centrifugation and washed with water until getting neutral, and then dried at 103°C.

2.3. Composition and properties of thesitinakite

The synthesized sample was studied using X-ray diffraction (diffractometer XRD-6000 Shimadzu with CuKα radiation in the range of reflection angles 2θ of 2 to 60°), infrared spectroscopy (spectrometer IR-Prestige 21 Shimadzu ranging 400–4000 cm^{-1}), and scanning electron microscopy (high-resolution scanning microscope Tescan Vega 3 LMH and Tescan MIRA 3 LMU equipped with Oxford Instruments X-ACT energy dispersive analyzer), thermal analysis (DTG 60 Shimadzu, temperature range 25 to 1000 °C, heating rate 10 °C/min, air environment). Adsorption and textural properties were evaluated by low-temperature (–196 °C) nitrogen adsorption-desorption as measured by the volume method on a NOVA 1200e (Quantachrome) surface area and porosity analyzer. The pore surface area per unit mass of solid phase, or specific surface, was determined by the BET method. The single-point method was used to calculate both adsorption pore volume (V_{spads}) and adsorption average pore diameter (D_{spads}). The differential distribution of the mesopore volume by diameter (dV/dlgD) was calculated by the Barrett-Joyner-Halenda (BJH) method. The relative error in determining the pore volume was ± 1%, surface area and pore size ±10%. Prior to analysis, samples were degassed in vacuum for 2 h at 110°C. The zeta-potential and pH of the isoelectric point were measured using a Zetasizer Nano ZS equipment (Malvern Instruments Ltd). The measurements were carried out in the presence of a background electrolyte (0.001 M NaCl) in the pH range from 2 to 10 incrementing by 1 (sample weight 0.005 g, solution volume 10 mL).

2.4. Study of sorption processes

Sorption of Sr^{2+} and Ba^{2+}

Sorption was carried out under static conditions using polypropylene dishes. A sitinakite probe was treated with a solution having an exact content of a particular cation (solid and liquid phase ratio of 1:500) and kept for 24 hours with occasional shaking. Upon completing the experiments, the solution was centrifuged and an aliquot was taken. The determination of initial (C_0) and equilibrium (C_p) cation concentrations was performed by atomic emission spectroscopy on inductively coupled plasma with a Vista MPX Rad spectrometer. The effect of the initial concentration, temperature (from 20 to 100°C), pH of the solutions (from 2 to 8, adjusted by HCl and NH_4OH), and background electrolyte on the adsorption capacity of titanosilicate was estimated.

Sorption of NH^{4+}

Determination of the sorption capacity for the NH^{4+} cation was carried out using the calorimetric method (using the Nessler reagent). The concentration of ammonium chloride was 100 mg/L, pH of the solution was 5.55±0.1, the length of the experiment was 10, 20, 30, 40, 50, and 60 minutes.

Sorption of radionuclides

In batch experiments, 1 g of sample was added to a glass beaker containing 20 mL of the solution and then aged at room temperature for 24 h under static conditions. The solutions were prepared by mixing standard solutions of U^{238}, Th^{232}, Ra^{226}, and distilled water. The concentrations of radionuclides in model solutions were higher than their concentrations in natural water, which commonly contains between $n\times10^{-8}$ and $n\times10^{-5}$ g/L uranium; thorium content is typically less than $n\times10^{-8}$ g/L, radium content ranges from $n\times10^{-14}$ to $n\times10^{-11}$ g/L [50]. The pH of the solution varied in the range 6.8–7.0 (adjusted with NH_4OH) and changed insignificantly during the sorption process. The choice of acid-alkaline conditions to saturate the sorbent was based on a process

occurring in the environment. According to Aleksahin [51], such conditions allow the continued existence of the mono- and polynuclear hydrolyzed forms of UO^2OH^+, $ThOH_3^{5+}$, $Th_2(OH)_3^{5+}$, $Th_4O_8^{8+}$, $(UO_2)_3(OH)_5^+$; radium in solution is in the form of Ra^{2+}. After the sorption test samples were separated from liquid by filtering.

Uranium content was determined by the luminescence method (sensitivity 2.0×10^{-8} g/g, measurement error 20%) [52]. Thorium was determined photocolorimetrically from arsenazo III (method sensitivity 1.0×10^{-8} g/g, measurement error 20%) [53]. Radium was determined using the emanation method (sensitivity 2.0×10^{-12} g/g, measurement error 15%) [54]. Intensity of absorption was estimated by the content of radionuclides in the extracts as obtained from a three-stage treatment of the sorbent enriched with radionuclides consequently using distilled water, 1M ammonium acetate (CH_3COONH_4) and 1M hydrochloric acid (HCl). In all tests, the amount of extractant was 20 cm^3 and extraction time was 24 h.

2.5. Computational details

To get additional molecular level insight into the adsorption behavior of sitinakite, periodic DFT calculations were carried out at the PBE+U [55] and the projector augmented wave (PAW) [56,57] level of theory as implemented in VASP 5.2 [58-61]. All calculations were spin-polarized and the energy cutoff was set to 500 eV. Following the Dudarev description model, the defined Hubbard (U) parameters were set to 9.3 eV for Ti[62] and 4.5 eV for U [63]. The k-point grid sampling using Monkhorst-Pack mesh of 3x3x3 was provided [64]. Convergence was assumed to be reached when the forces acting on each atom were below 0.05 $eV\cdot Å^{-1}$.

Results and discussion

3.1. Synthesized sitinakite

As a result of the hydrothermal synthesis, white powders containing well-formed cuboidal and short-prismatic crystals with a size of 0.1–3 μm (Figure1a, b) were obtained. The HRTEM image of the sample (Figure1c,d) illustrates that the powder is polycrystalline, which according to the XRD analysis could be assigned to a structure similar to the natural mineral sitinakite (Figure 2a).The crystal structure of sitinakite (Figure 2b) comprises chains of TiO_6octahedra elongated along the "c" axis and combined into a frame by isolated SiO_4 tetrahedra [65]. The porous system consists of narrow channels (2.3 Å in diameter) parallel to the "c" axis. These channels are filled with Na^+ and K^+ cations as well as water molecules. Nitrogen physisorption shows that our sitinakite material has a low specific surface area (from 40 to 50 m^2/g), pore volume of 0.08 cm^3/g, micropore volume of 0.027 cm^3/g, and average pore radius of 2.2nm (Figure 1f). Thermogravimetric analysis showed that the total weight loss is 14.8% (Figure 1e).When heated to 175°C, physically adsorbed water is removed first and the weight loss is 4.2%. Further increase in temperature to 300 °C leads to the removal of hydrate water associated with exchangeable cations, and the weight loss is 7%.

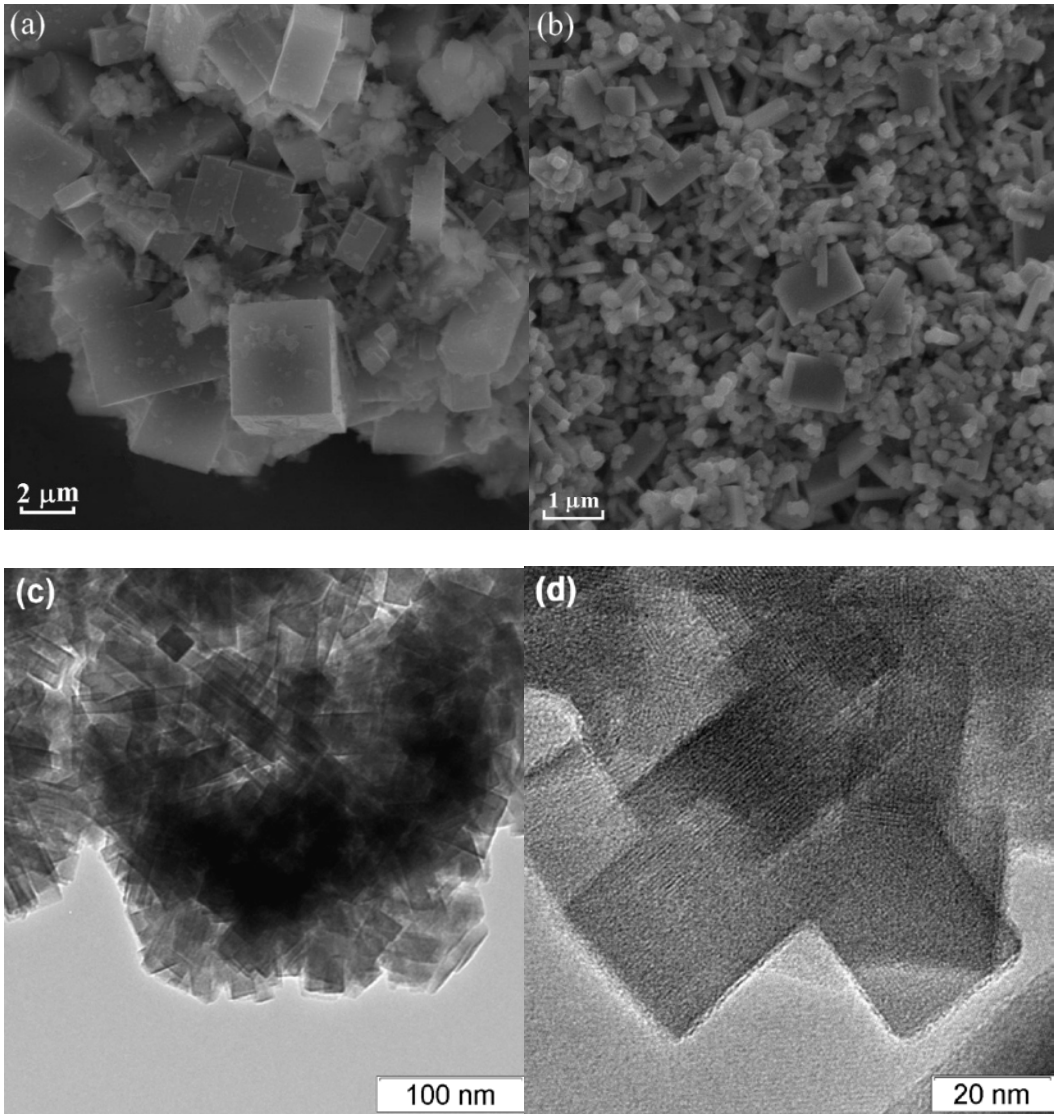
(a)
2 μm
(b)
1 μm
(c)
100 nm
(d)
20 nm

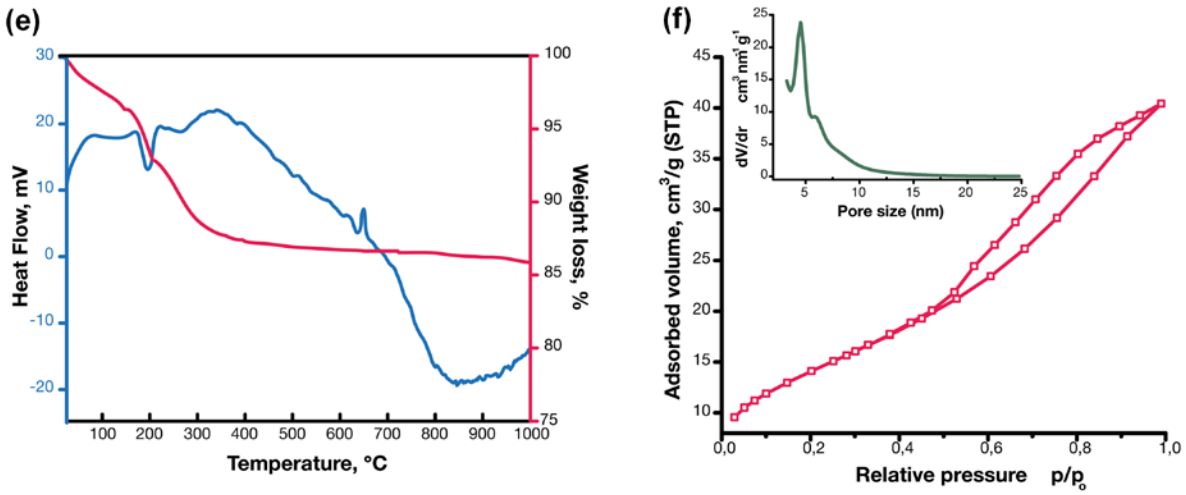
(e)
Heat Flow, mV
Weight loss, %
Temperature, °C
(f)
Adsorbed volume, cm³/g (STP)
dV/dr cm³ nm⁻¹ g⁻¹
Pore size (nm)
Relative pressure p/p₀

Figure 1. SEM (a, b) and TEM (c, d) images of the synthesized sitinakite; DTA (red curve) and TG (blue curve) curves of as-synthesized sitinakite (e); nitrogen physisorption isotherms (pink curve) and pore size distribution (green curve) (f).

XRD study of samples calcined at 200 and 300 ºC showed that significant changes of sitinakite structure do not occur; the intensity of the main reflexes slightly reduced (Figure 2a). The decrease of the mass by 3.6% in the range from 300 to 1000 ºC is associated with an irreversible loss of structural water, leading to the destruction of the sitinakite lattice with a concomitant strong fixation of Na^+ cations within the framework. The calcination at 600°C results in the amorphization of the material as is evident from the loss of the reflexes in the XRD patterns (Figure 2a). An exothermic peak at 650 ºC in the DTA curve corresponds to the crystallization of a new phase that is identified as the freudenbergite (Figure 2a, c). The low degree of crystallinity of the sample, even after annealing at 650 and 700°C, is explained by the short isothermal exposure time.

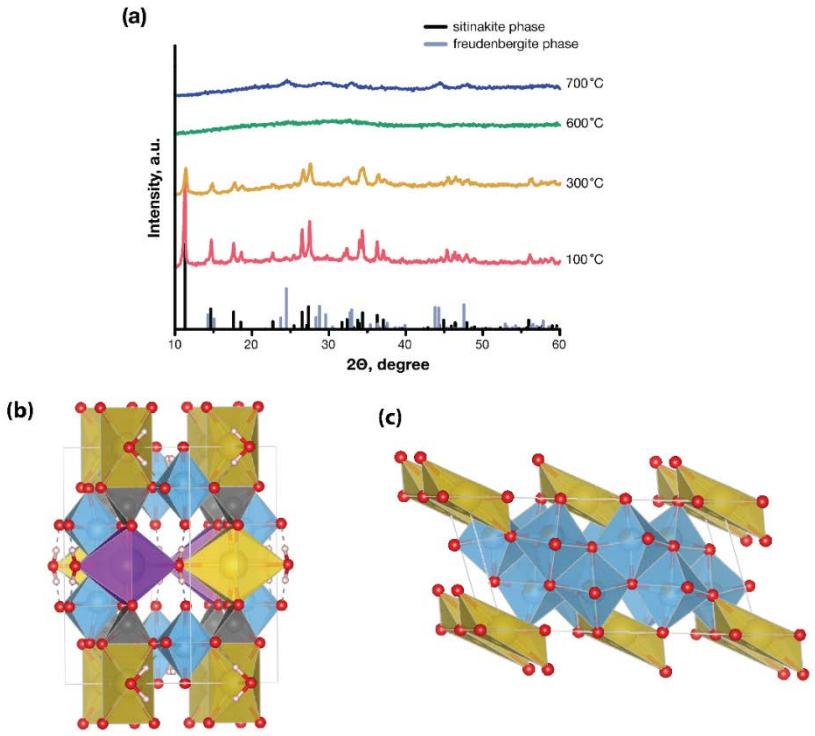

Figure 2. XRD patterns of the synthesized sitinakite calcined at 100, 300, 600 and 700 °C (a); crystal structure of sitinakite (b), crystal structure of freudenbergite (c) (titanium is blue, silicon is grey, oxygen is red, hydrogen is pink, sodium is yellow, potassium is purple).

The high thermal stability of sitinakite (up to 300 °C) renders the synthesized materials potentially suitable for the efficient utilization of its ion exchange properties, even when operating under harsh conditions commonly encountered in the nuclear energetics. For example, the temperature of spent nuclear fuel in separate layers is about 130 °C [66]. Previous studies suggest that the exchange capacity of natural sitinakite can be enhanced at relatively high temperatures (100–150°C)[67].

The most promising approach for reprocessing irradiated fuel in the nuclear fuel cycle is immobilization of radionuclides in the composition of mineral-like ceramics of SYNROC type.

The freudenbergite phase, obtained during the recrystallization of sitinakite up to 1000 ºC, can be attributed to the SYNROC type of ceramics [68, 69].

3.2. Sorption characteristics for Ba^{2+} and Sr^{2+}

3.2.1. Effect of the pH of the solution and sorption mechanism

A set of experiments on Sr^{2+} sorption under static conditions (at 20°C, 24 h) and in the pH range from 2 to 8 showed that sorption capacity increases rapidly on passing from acidic to alkaline medium which indicates slightly acidic characteristic of sitinakite as a sorbent (Table S2).

Measurements of the surface charge of titanosilicate (Figure 3) showed that particles in the pH range 2 to 2.7 have a positive charge. Due to the fact that under these conditions the charges of sitinakite and Sr^{2+} have the same sign, they are subject to the forces of electrostatic repulsion. In the pH range 2.7 to 10.0 the surface is negatively charged and compensated by counter-ions, Na^{+} cations. When pH is greater than 2.7 (pH of the isoelectric point), the sodium cations included in the titanosilicate structure upon contacting the solution can be desorbed from the surface and replaced by other ions of the same sign, in particular, Sr^{2+} cations. It is confirmed by the determination of sodium concentration in the solution after the sorption equilibrium is reached (Table S2).

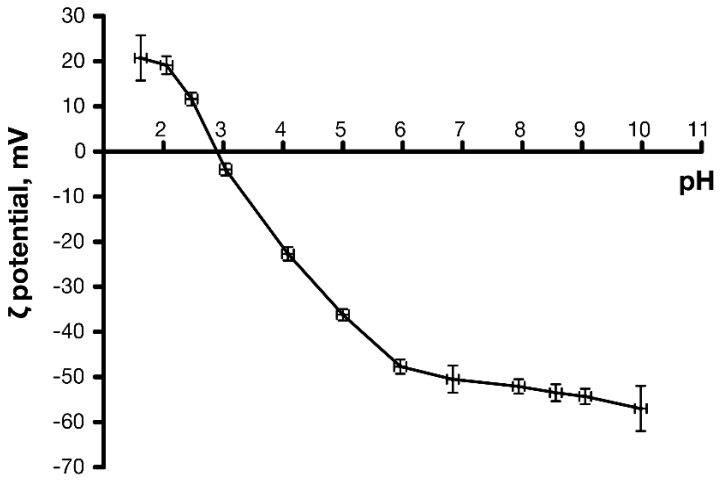

Figure 3. Dependence of the zeta potential (ξ) of sitinakite surface on the pH of the solution.

The low sorption capacity of titanosilicate in a weakly acidic medium with a negative surface charge can be associated with competitive capture of free ion-exchange sites by counter-ions H^+ due to their higher concentration in the acidic medium, and also with the destruction of the titanosilicate framework.

Acid resistance of titanosilicate was tested using a solution of HCl (0.01, 0.1, 1.0 M) and phase contact time of 24 hours. Unit cell parameters calculated according to the X-ray analysis (Table S3, Figure S1) indicate that the crystal lattice is compressed due to the replacement of larger cations (Na^+) with smaller ones (H^+). The parameters of the titanosilicate cell after sorption of Sr^{2+} and Ba^{2+} at various temperatures were calculated as well. It is evident that when the Na^+ cation is replaced with larger cations, the opposite effect, i.e., an increase in lattice parameters, is observed. This fact indicates that the most likely mechanism of sorption on titanosilicate is ion exchange.

3.2.2. Adsorption isotherms for Sr^{2+}

The amount of absorbed strontium increases with its concentration in the initial solution, and the maximum of sorption capacity is 27.5 mg/g (0.64 meq/g). The resulting isotherm was analyzed using the Langmuir and Freundlich models [71]. An adsorption isotherm plotted at varying concentrations of strontium is shown in Figure S2. The Langmuir model is used to describe adsorption on a homogeneous surface with little interaction between the adsorbed molecules. According to the model, there is uniform adsorption energy on the surface, and the maximum adsorption depends on the level of saturation of the monolayer. The Freundlich model is used to describe the processes of sorption of substances on a single heterogeneous sorbent layer with an undetermined number of active binding sites. The feature of this model is the impossibility of calculating the maximum sorption capacity (number of active sites per unit coupling agent).

Table 1 shows the calculated parameters and correlation coefficients of the equations. Both models completely correlate with one another. The value of R^2 for the Langmuir model is slightly higher than that for the Freundlich one, suggesting the predominance of monomolecular adsorption. The Freundlich isotherm factor n is greater than 1, indicating a decrease in binding energy as the surface is filled.

Table 1. Constants and correlation coefficients for the adsorption models by Langmuir and Freundlich.

Langmuir model			Freundlich model		
q_m, mg/g	$K_L \cdot 10^{-3}$, L/mg	R^2	n	K_F, mg/g $(L/mg)^{1/n}$	R^2
29.42	21.4	0.9875	3.60	4.315	0.9123

3.2.3. Effect of temperature on the adsorption of strontium ions

The temperature effect on the sorption of Sr^{2+} ions from aqueous solutions was studied at optimal pH values (Table S4). The results showed that increasing temperature in the range from 20 to 100 °C enhanced the sorption capacity from 27 to 44 mg/g at pH=6 and from 33 to 58 mg/g at pH=8. It should be noted that at 100°C there is no drop in the sorption capacity value, which confirms the thermal stability of titanosilicate.

Increase in sorption activity with rise in temperature indicates the endothermic nature of the process. If one considers titanosilicate to be a weak electrolyte formed by a strong base and a very weak insoluble titano-silicic acid $H_{2(x+y)-z}Ti_xSi_yO_z \cdot nH_2O$, then rising solution temperature should increase the degree of dissociation of the functional groups and, consequently, the ion exchange capacity of the product. This assumption is suitable for the sorption of strontium at pH = 8, where the increase in the concentration of sodium cations desorbed into the solution is noted. For solutions with pH = 6 sodium concentration remains unchanged. Thus, we can assume the presence of a mixed sorption mechanism, involving both cation-exchange mechanism (Figure 4a) and specific sorption (Figure 4b) due to unfulfilled electrical connections of lattice ions at the interface and/or the presence of functional (-OH) groups related to Ti-OH in the channels of titanosilicate.

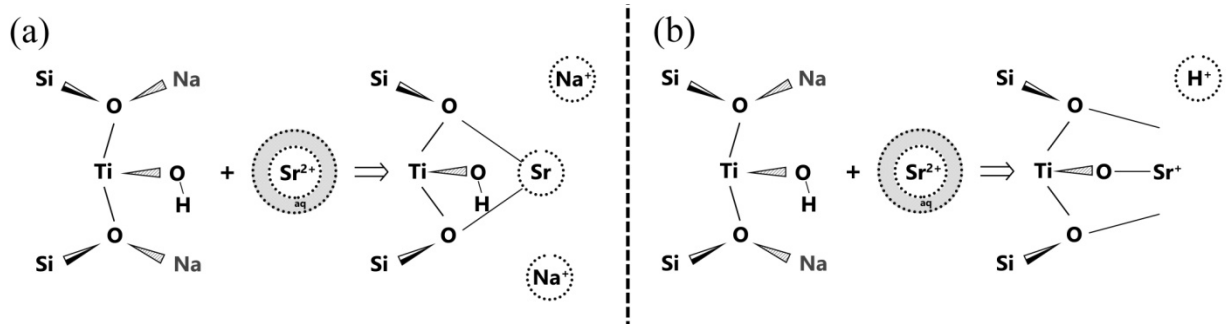

Figure 4. Scheme of hypothetical sorption mechanism on the sitinakite: a – cation-exchange mechanism, b – specific sorption.

To clarify the sorption mechanism of Sr^{2+} by titanosilicate, we studied IR spectra of the original sample and those after adsorption at 20, 60, and 100 °C (pH=6). The spectrum of the original sample (Figure 5) is similar to the spectrum of natural titanosilicate [70, 72].

The region of stretching vibrations of the OH bond reveals several absorption bands with maxima at 3205, 3340, and 3530 cm^{-1}. A weak absorption maximum at 3530 cm^{-1} is associated with the OH–Si vibrations [73].The bands at 3205 and 3340 cm^{-1} belong to the stretching vibrations of the water molecule and the band at 1630 cm^{-1} to its bending vibrations. A weak absorption maximum at 1437 cm^{-1} is associated with the vibrations of Si-(OH) bonds. In Ref [74]. it is noted that the absorption band at 1400–1450 cm^{-1} corresponding to the bending vibrations of OH groups in the vertices of silicon-oxygen tetrahedra is a distinctive feature of silicates. Characteristic absorption bands in the region from 400 to 1000 cm^{-1} (430, 443, 471, 575, 778, 902, 970) are the vibrations of the Si–O, Ti–O, Ti–O–Ti, Si–O–Si, Ti–O–Si bonds. In particular, the band at 471 cm^{-1} is attributed to the bending vibrations of Si–O–Si [74-76], and that at 778 cm^{-1} to the symmetric stretching vibrations of Si–O–Si typical for silicon in the SiO_4 tetrahedron [77]. Absorption bands with maxima at 900 and 970 cm^{-1} correspond to the stretching vibrations of non-bridging Si–O bonds in various silicate groupings (Si–OH, Si–O–Ti, Si–O), and that at 430 cm^{-1} to the bending vibrations of Si–O. The band with a peak at 575cm^{-1} is attributed to the stretching Ti–O–Ti vibrations [76].

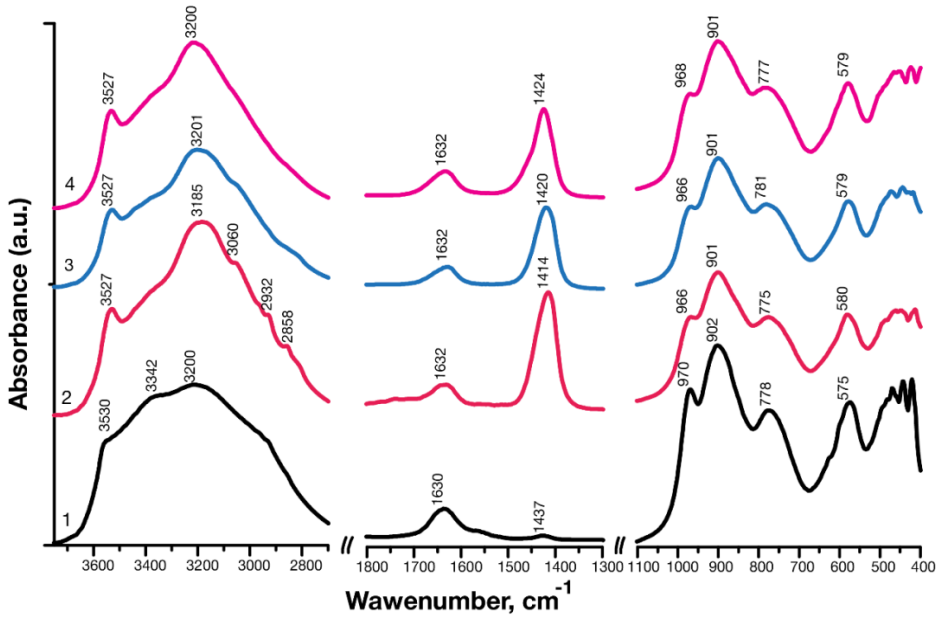

Figure 5. IR spectra of titanosilicate: 1 – initial sample; 2 – saturated with Sr^{2+} at 20 °C; 3 – at 60 °C; 4 – at 100 °C.

After sorption of Sr^{2+} at 20, 60, and 100°C the characteristic region (400–1100 cm^{-1}) has no significant changes. The appearance of an intensive peak at 1430 cm^{-1} and weak absorption bands at 2858, 2931 and 3067cm^{-1} correspond to the bending and stretching vibrations of the NH_4^+ group. It is also evident that compared to the initial sample the maximum peak at 3200 cm^{-1} corresponding to the OH vibrations of water molecules is sharpened. The NH_4^+smectites where water is coordinately linked to the NH_4^+ cations, except for the main NH_4^+absorption at 3270 cm^{-1}, are characterized by additional absorption bands at 3067 and 2855 cm^{-1} due to hydrogen bonds between NH_4^+ and water. As water is removed, these additional bands weaken and merge into a diffuse absorption band, whereas the band at 3270 cm^{-1} is sharpened and amplified. The adsorption of Sr^{2+} is accompanied by the process of adsorption of NH_4^+, due to the solution alkalization with

NH_4OH. To confirm this, the experiments on extracting the ammonium cation were carried out. According to the obtained data, the sorption capacity of titanosilicate was 18 mg/g (1meq/g).

The experiments on the sorption of Sr^{2+} from the solution where pH was adjusted without using external electrolytes were also carried out. Sorption was carried out at 20, 60, and 100°C for 24 hours, the pH of the solution was 4.70 ±0.10.

As in our previous experiments, a rise in temperature leads to an increase in sorption capacity, as well as the number of desorbed Na^+ cations indicating the increased degree of dissociation of functional groups (Table 2). A decrease in pH at higher temperatures could be an indirect indication of the replacement of H^+ cations with Sr^{2+}. In Ref. [18] it was established that sitinakite-like titanosilicate $H_2Ti_2O_3SiO_4 \cdot 1.6 \cdot H_2O$ effectively absorbs cations of Cs and Rb even at pH < 1, which indicates the existence of a strongly acidic functional group bonded to the Ti–OH groups.

Table 2. Sorption capacity of titanosilicate for the Sr^{2+} cation.

(solution volume 0.015 L, sample mass 0.03 g, C_0 1000 mg/L)

T,°C	C_p, mg/L	pH		Sorption capacity		Amount of desorbed Na, meq/g
		before	after	mg/g	meq/g	
20	838.9	4.70 ± 0.10	7.04±0.10	80.53	1.78	1.65
60	824.5	4.70 ± 0.10	6.30±0.10	87.75	2.00	1.74
100	804.8	4.70 ± 0.10	6.05±0.10	92.60	2.23	1.86

3.2.4. Effect of temperature on the adsorption of barium ions

Table 3 shows the results of determining the sorption capacity of sitinakite for the Ba^{2+} cation at temperatures of 20, 60, and 100°C. With rising temperature, the sorption capacity for Ba increases, revealing at the same time a decrease in pH and the lack of Na^+ cations.

Table 3. Sorption capacity of titanosilicate for the Ba^{2+} cation.

(solution volume 0.015 L, sample mass 0.03 g, C_0 1000 mg/L)

T, °C	C_p, mg/L	pH		Sorption capacity		Amount of desorbed Na, meq/g
		before	after	mg/g	meq/g	
20	773.4	5.59±0.10	6.10±0.10	113.30	1.65	1.70
60	741.9	5.59±0.10	5.48±0.10	129.75	1.88	1.71
100	721.7	5.59±0.10	5.28±0.10	139.10	2.03	1.81

3.2.5. SEM-EDX analysis

EDX analysis of sitinakite showed that the adsorption of Sr^{2+} and Ba^{2+} cations is characterized by their uniform distribution across the surface of the sorbent (Figure 6, S3).

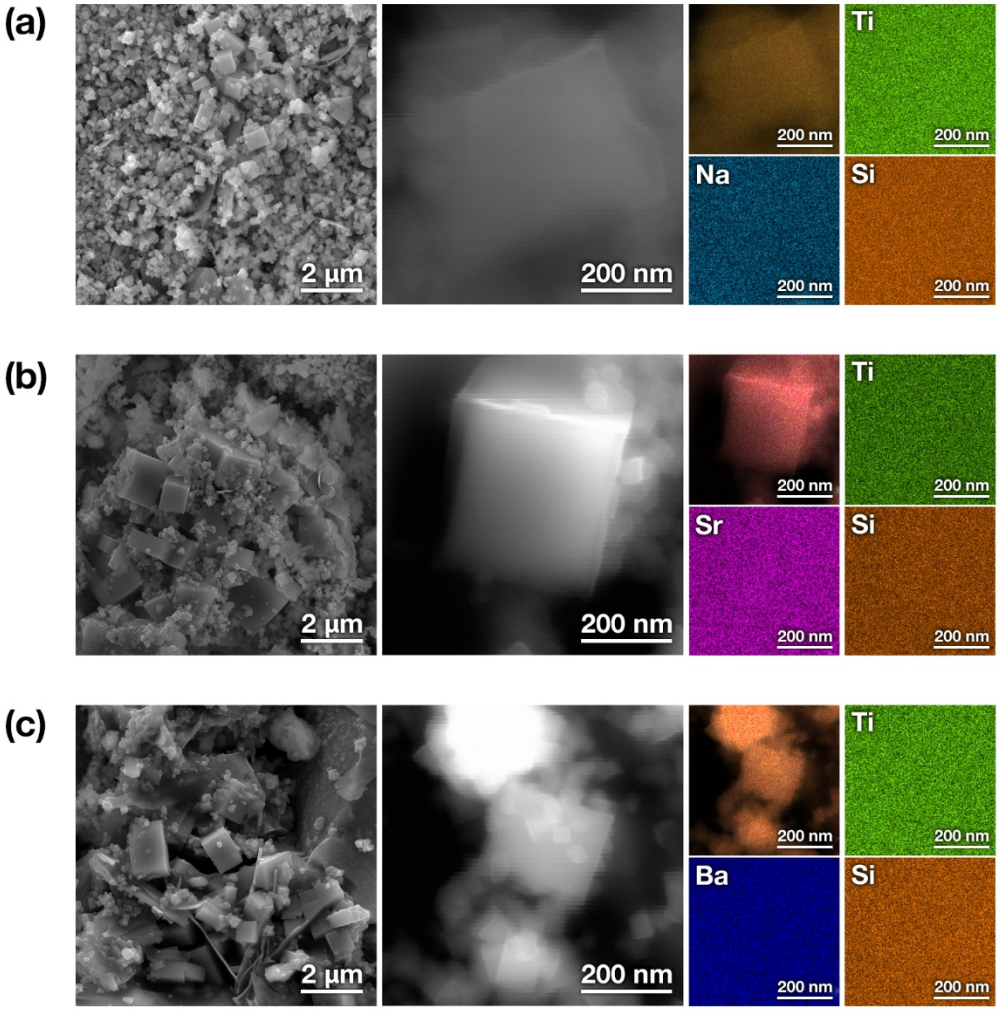

Figure 6. SEM images and EDS mapping of sitinakite powder: a – initial sample; b – after adsorbing Sr^{2+} at 20°C; c – after adsorbing Ba^{2+} at 20 °C.

3.2.6. Thermodynamics of the sorption process

Data on the temperature dependence of the cation sorption on sitinakite were used to calculate the thermodynamic sorption parameters ΔH °, ΔS °, and ΔG ° using the fundamental equations [78]:

$$lnK_d = -\frac{\Delta H^\circ}{RT} + \frac{\Delta S^\circ}{R} \quad (1)$$

$$\Delta G^\circ = \Delta H^\circ - T\Delta S^\circ \quad (2)$$

$$\Delta G^\circ = -RTlnK_d \quad (3)$$

where ΔH◦,ΔS◦,ΔG◦ and T are, respectively, the enthalpy change, entropy change, Gibbs free energy of adsorption and absolute temperature in K; R is the universal gas constant (8.314 Jmol−1 K−1); K_d is the adsorption equilibrium constant.

Enthalpy change was calculated from the slope of straight line plot between log K_d and 1/T derived from application of the van't Hoff equation in linearized form (Eq.4).

$$lnK_d = -\frac{\Delta H^\circ}{RT} + const \quad (4)$$

Table 4 shows the thermodynamic parameters calculated from above given equations. Enthalpy change, obtained was $\Delta H°=3.14$ kJ·mol^{-1}for Ba^{2+}, and $\Delta H°=2.63$ kJ·mol^{-1} for $Sr^{2+}$where positive value indicates an endothermic nature of theadsorption process.

The endothermicity of sorption is due to the energy expended on the rupture of the hydrate shell of Ba and Sr cations in solution. At the same time, energy expenditure exceeds the exothermic effect of the process of cation addition to titanosilicate.

Enthalpy values not greater than 30 kJ/mol for all cationes indicate ion exchange to be the adsorption mechanism. Positive entropy values are also associated with dehydration of ions and emergence of larger amounts of free molecules of water (increased randomness at the solid phase – solution boundary in the process of cation sorption) [79, 80].

Negative values of Gibbs energy show that the process is spontaneous. The selectivity of sorption increases from Ba to Sr, and an increase in Gibbs energy with increasing temperature indicates that sorption is preferable at high temperatures.

Table 4. Thermodynamic parameters of sorption.

Cation	Temperature, K	ΔG, kJ/mol	ΔH, kJ/mol	ΔS, J/mol·K
Ba^{2+}	293	-12.16	3.14	52.20
	333	-14.25		
	373	-16.36		
Sr^{2+}	293	-11.10	2.63	46.86
	333	-12.97		
	373	-14.84		

3.2.7. Effect of a third-party electrolyte on the sorption capacity of titanosilicate

The selectivity of sorbents in the presence of salts and other components contained in aqueous media plays an important role in sorptive extraction. For example, synthetic zeolites NaA and NaX are widely used as sorbents, which can effectively remove strontium and cesium from solutions with low concentrations. However, their selectivity to radionuclides decreases with increasing concentrations of competing ions. Therefore, we determined the characteristics of sorption of Sr^{2+} and Ba^{2+} from the solutions containing extraneous ions, Na^{+} (0.1 M). An insignificant decrease in sorption capacity indicates high selectivity of titanosilicate towards these ions (Table 5).

Table 5. Sorption capacity of titanosilicate in the presence of a background electrolyte.

Cation	Concentration of competing ion Na^+	Sorption capacity q_e	
	mol/L	mg/g	meq/g
Sr^{2+}	0.1	64.85	1.48
Ba^{2+}	0.1	91.71	1.34

3.3. Sorption of radionuclides

The results (Table 6) show that titanosilicate exhibits selectivity towards all tested radionuclides, with the degree of extraction for uranium and radium reaching almost 99 %. Only for thorium this figure was slightly lower, about 82 %.

Table 6. Sorption and sorption strength of natural radionuclides

Radionuclide	Initial radionuclide content of the solution, g	Solution content after exposition, g	Extraction degree, %	Degree of desorption, % of the adsorbed amount, by		
				Deionized water	1M ammonium acetate	1 M hydrochloric acid
Thorium-232	$8.45 \cdot 10^{-6}$	$1.51 \cdot 10^{-6}$	82.1	1.6	4.7	55.2
Uranium-238	$11.30 \cdot 10^{-6}$	$0.14 \cdot 10^{-6}$	98.8	0.4	0.7	60.3
Radium-226	$7.29 \cdot 10^{-10}$	$0.09 \cdot 10^{-10}$	98.8	0.75	0.05	28.4

Another important characteristic of radionuclide sorption is its absorption strength. As noted above, the absorption strength was evaluated by radionuclide content in the sequentially obtained extracts. This study showed that 60.3 and 55.2% of the absorbed amount of uranium and thorium radionuclides can be desorbed while treating the sorbent with a hydrochloric acid solution. For radium this figure is only 28%. This can be explained by the fact that the sorption of the radium cation whose radius is 1.44 Å (the smallest of all tested radionuclides) is accompanied by the diffusion of the radionuclide into the sorbent, making its holding tighter.

3.4. Model DFT calculations

Here we considered an ion exchange model of the parent sodium form of sitinakite with Ra^{2+}, UO_2OH^+, $Th(OH)_3^+$, Sr^{2+}, Ba^{2+} cations. The free cationic complexes were approximated as the respective aqua complexes. Three periodic sitinakite models with varied degree of hydration were considered in this study to assess the sitinakite structural specificity (polyhedral representation in Figure7).

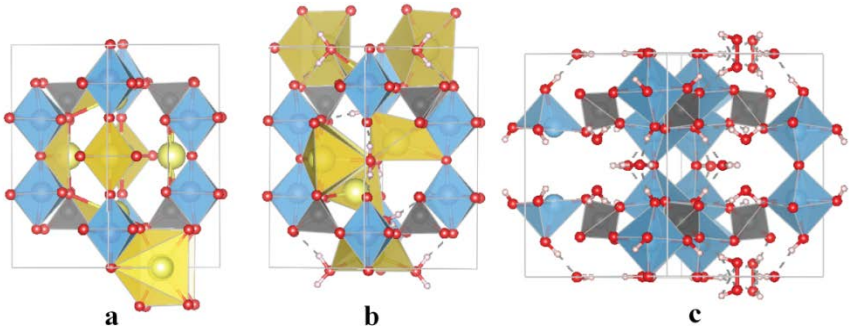

Figure 7. Models of sitinakite unit cells: a – Na-sitinakite, b – aqua Na-sitinakite, c – aqua H-sitinakite (oxygen atoms are red, titanium atoms are blue, silicon atoms are grey, sodium atoms are yellow).

These models were used to probe the respective proton- and sodium exchange mechanisms proposed above. The Na-exchanged models (*a* and *c*) correspond to the natural sitinakite structural parameters investigated in the current study where an octahedral coordination of tetravalent Ti atoms generates negative charges (Na-sitinakite, aqua Na-sitinakite in Figure7). System electroneutrality is balanced by exchangeable Na^+ whose presence leads to larger lattice parameters compared to natural sitinakite (Table 7). The *aqua Na-sitinakite* accounts for the effect of water molecule solvation. The *aqua H-sitinakite* model is the representation of the proton-

exchanged sitinakite where the negative charges are compensated by H^+. Below we focus on the energetics of both ion-exchange mechanisms performed on the modeled unit cells and adsorbed ion coordination in the environmentally diverse sitinakite unit cells.

Table 7. Lattice parameters of relaxed sitinakite models.

Sitinakitemodel	Latticeparameters, Å		
	a	*b*	*c*
Naturalsitinakite	7.819	7.819	12.099
Na-sitinakite	7.987	7.972	12.165
aquaNa-sitinakite	7.960	7.956	12.120
aqua H-sitinakite	11.249	11.436	12.161

Sr, Ba and Ra sorption

The Ba^{2+} and Sr^{2+} ions show similar coordination behavior in all models and therefore will be described simultaneously (Figure 8). Our model DFT simulations qualitatively confirmed the experimentally established endothermicity of the Sr^{2+} and Ba^{2+} sorption. The relative favorability of the process is calculated for the Na-exchanged models where the sorption is primary ionic and based on stronger bonding of divalent cations than monovalent ones. In case of Na-exchange unit cells (a and b), the energetic effects of Sr^{2+} sorption are 1 and –9 kJ/mol, while Ba^{2+} sorption has stronger endothermic effects of 19 and 97 kJ/mol due to the larger hydrated ionic radius. The energetics of proton exchange by Sr^{2+} and Ba^{2+} ions is 166 and 135 kJ/mol (c model) that is in line with the purely Coulombic nature of their sorption. Both ion-exchange mechanisms display higher selectivity towards Ra^{2+} sorption with energetic effects of –108, –212 and –15 kJ/mol for a, b and c unit cells, respectively (Table 8).

Table 8. Adsorption energies (kJ/mol) of cations for different sitinakite models

Unitcellmodel	Sr^{2+}	Ba^{2+}	Ra^{2+}
a	1	19	-108
b	-9	97	-212
c	166	135	-15

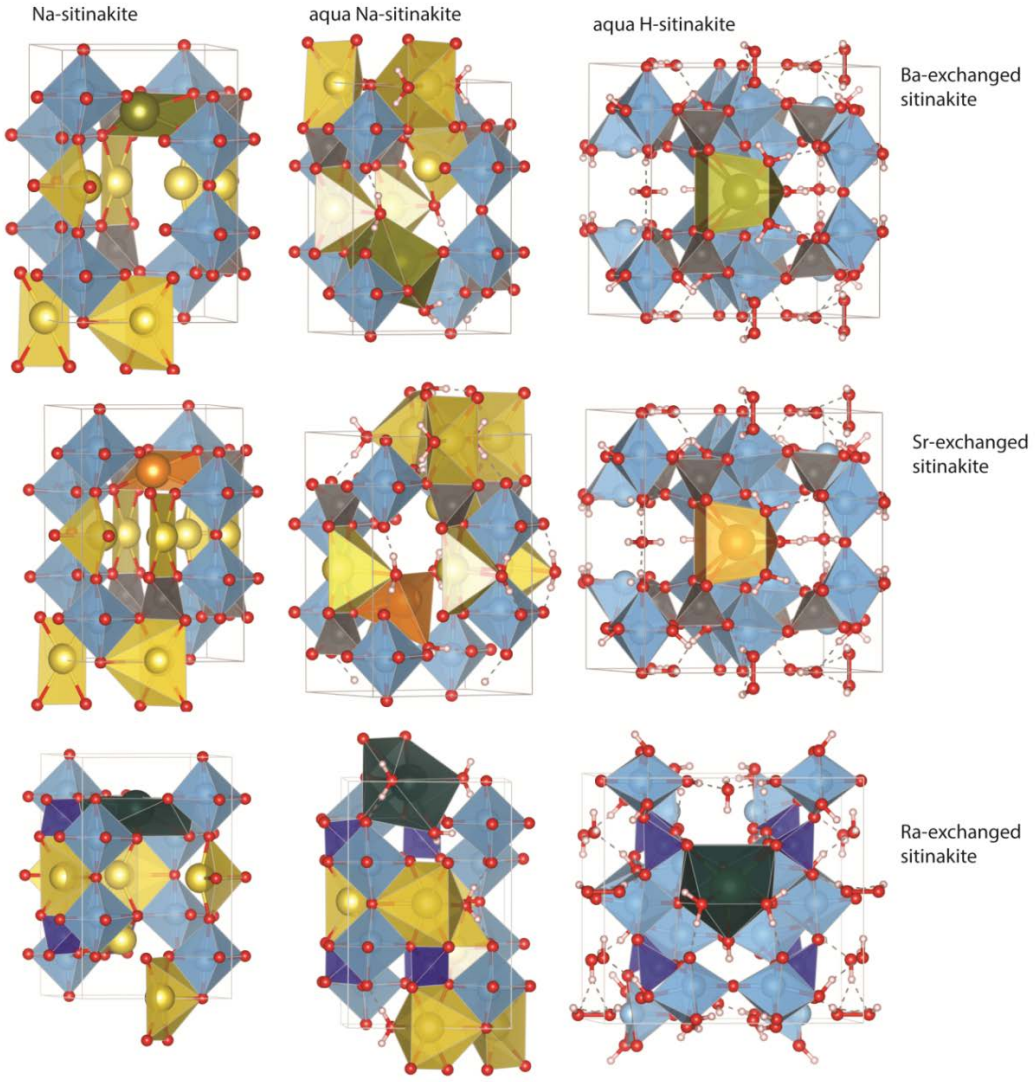

Figure 8. Ba^{2+}, Sr^{2+} and Ra^{2+} ion-exchange sorption on the Na-sitinakite, aqua Na-sitinakite and aqua H-sitinakite unit cell models.

U and Th sorption

U- and Th-exchanged unit cells were modeled considering the dominant existing cationic forms at experimental pH values of 6–7 (Figure 9).

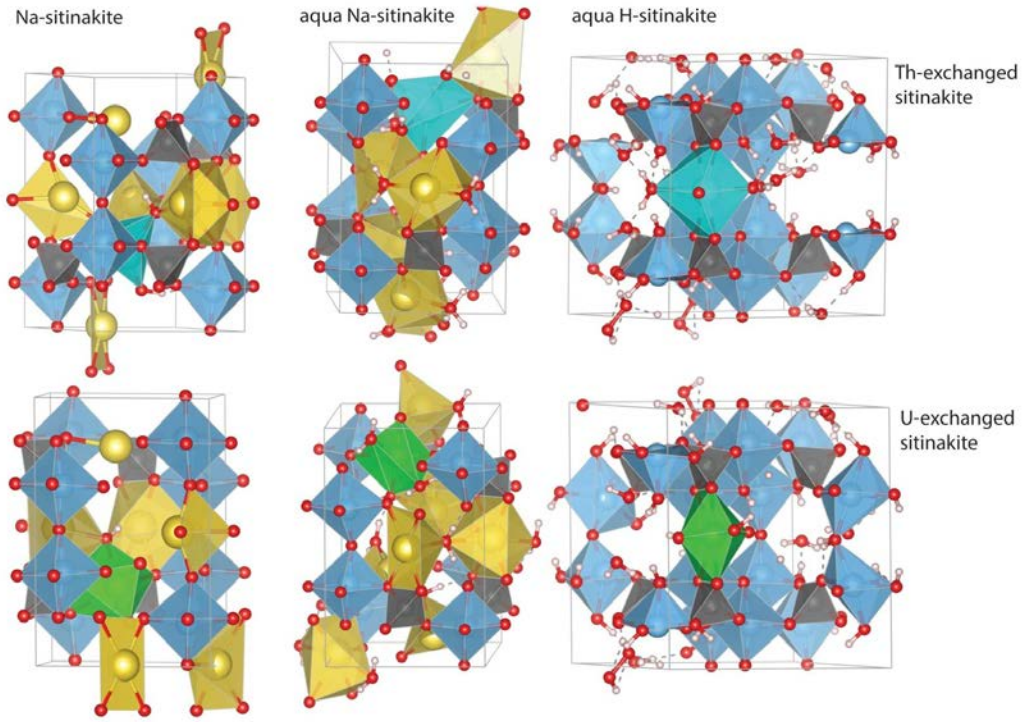

Figure 9. UO_2OH^+ and $Th(OH)_3^+$ ion-exchange sorption on the Na-sitinakite, aqua Na-sitinakite and aqua H-sitinakite unit cell models.

Table 9. Adsorption energies (kJ/mol) of cations for different sitinakite models.

Unit cell model	UO_2OH^+	$Th(OH)_3^+$
a	-50	-297
b	-164	-116
c	-162	-57

The most probable hydrolytic products were considered to be $Th(OH)^{3+}$ and $UO_2(OH)^+$ [81, 82]. The enthalpies of the UO_2OH^+ adsorption exhibit strong exothermicity with effects of –50, –164 and –162 kJ/mol, while $Th(OH)^{3+}$ adsorption stabilized with exothermic effects of –297, –116 and

–57 kJ/mol for a, b and c models, respectively (Table 9). The imposed energetic favorability is supposedly related to the change of interatomic bonding to covalent type.

4. Conclusions

A highly selective adsorbent for multivalent cationic species based on a sitinakite-typetitanosilicatewas prepared hydrothermally from a leucoxene ore enrichment waste of the Yaregskoye deposit (Russia, Komi Republic). The synthesized material was used as for the selective removal of alkali-earth strontium (II) and barium (II) cations as well as the cationic species based on the natural isotopes of uranium, radium, and thorium from aqueous solutions. The influence of such parameters as pH, the initial concentration of the ions, and the presence of other electrolytes on the sorption parameters was investigated. The highest sorption capacity was obtained at pH> 3 and is 80 and 110 mg/g for Sr^{2+} and Ba^{2+}, respectively. Rising the sorption temperature to 100 °C leads to an increase in the sorption capacity to 92and 145 mg/g, respectively. The presence of a background electrolyte in the amount of 0.1 M (Na^{+}) does not affect the sorption capacity, which indicates a high selectivity of titanosilicate to Sr^{2+} and Ba^{2+} cations. The thermal stability makes it possible to use sitinakite under severe conditions, with a spent nuclear fuel temperature of 130 ° C

The thermodynamic analysis points to a spontaneous nature of the adsorption process. An increase in Gibbs energy upon increasing temperature indicates that sorption is preferable at high temperatures, and selectivity increases fromBa^{2+} toSr^{2+}. Enthalpy for all cations does not exceed 30 kJ/mol, thus confirming that the main process of adsorption utilizes the ion exchange mechanism. It should be noted that the ion exchange process is accompanied by adsorption due to functional hydroxyl groups, as indirectly indicated by decreasing pH of the solutions after sorption

at elevated temperatures. These Ti–OH hydroxyl groups, being strongly acidic, make a small contribution to the adsorption capabilities of titanosilicate, but allow the use at pH values above the isoelectric point (pH < 2.7).

Furthermore, the material shows a high selectivity towards radionuclides of radium, uranium, and thorium. By using the current titanosilicate materials, the extracting degree of over 99 % U and Ra, and 88 % Th could be achieved when extracting these species from their respective standard aqueous solutions. Radionuclides are strongly adsorbed by titanosilicate during water and ammonium acetate treatment; in an acidic medium desorption is 55–60 % for uranium and thorium, and 28 % for radium. The origin of the high adsorption selectivity for cationic complexes of thorium and uranium is rationalized based on periodic density functional theory calculations. The obtained results point to the described materials as promising and inexpensive sorbents for the selective extraction of radioactive isotopes and particularly those of Sr and Ba.

The proposed methodology can be used for the production of sorbents using enriched leucoxene ore waste disposal, which enables obtaining demanded functional materials in large volumes. Radionuclides saturated sitinakite can be transformed into ceramics of the SYNROC type at temperatures up to 1000°C for subsequent long-term burial.

Supporting Information.

Table S1. Chemical composition of hydrated precipitate, %.

SiO_2	TiO_2	Fe_2O_3	Al_2O_3	CaO	K_2O	$NbO+ZrO_2$
45.5	50.5	2.9	0.4	0.2	0.2	0.2

Table S2. Effect of pH on sorption properties of sitinakite.
(sorbent mass 0.02 g, solution volume 0.01 L, C_0=0 mg/L, pH is adjusted with NH_4OH and HCl)

Solution pH	Equilibrium concentration of Sr^{2+}, mg/L	Sorption capacity		Amount of Na^+ in the solution, meq/g
		mg/g	meq/g	
2.01 ± 0.10	47.4	1.30	0.03	~2.90
4.00 ± 0.10	45.9	2.05	0.05	~2.76
6.05 ± 0.10	23.7	13.15	0.30	~2.13
8.03 ± 0.10	16.7	16.65	0.38	~1.22

Table S3. Unit cell parameters of sitinakite.

Sample	a (Å)	b (Å)	c (Å)	Cell volume, $Å^3$
Natural sitinakite[68]	7.819	7.819	12.099	739.7
As-synthesized sitinakite	7.819±0.005	7.819±0.005	11.965±0.001	731.68±0.11
Synthesized sitinakite treated with 1M HCl	7.808±0.013	7.808±0.013	11.90±0.03	727.52±0.20
Sitinakite after sorption of Sr^{2+} (20 °C)	7.842±0.008	7.842±0.008	11.942±0.001	734.29±0.18
Sitinakite after sorption of Sr^{2+} (60 °C)	7.837±0.005	7.837±0.005	11.918±0.006	732.04±0.11
Sitinakite after sorption of Sr^{2+} (100 °C)	7.844±0.001	7.844±0.001	11.924±0.002	733.54±0.16
Sitinakite after sorption of Ba^{2+} (20 °C)	7.840±0.001	7.840±0.001	11.971±0.001	735.87±0.16
Sitinakite after sorption of Ba^{2+} (60 °C)	7.855±0.003	7.855±0.003	11.869±0.002	732.30±0.16
Sitinakite after sorption of Ba^{2+} (100 °C)	7.851±0.005	7.851±0.005	11.926±0.002	735.20±0.11

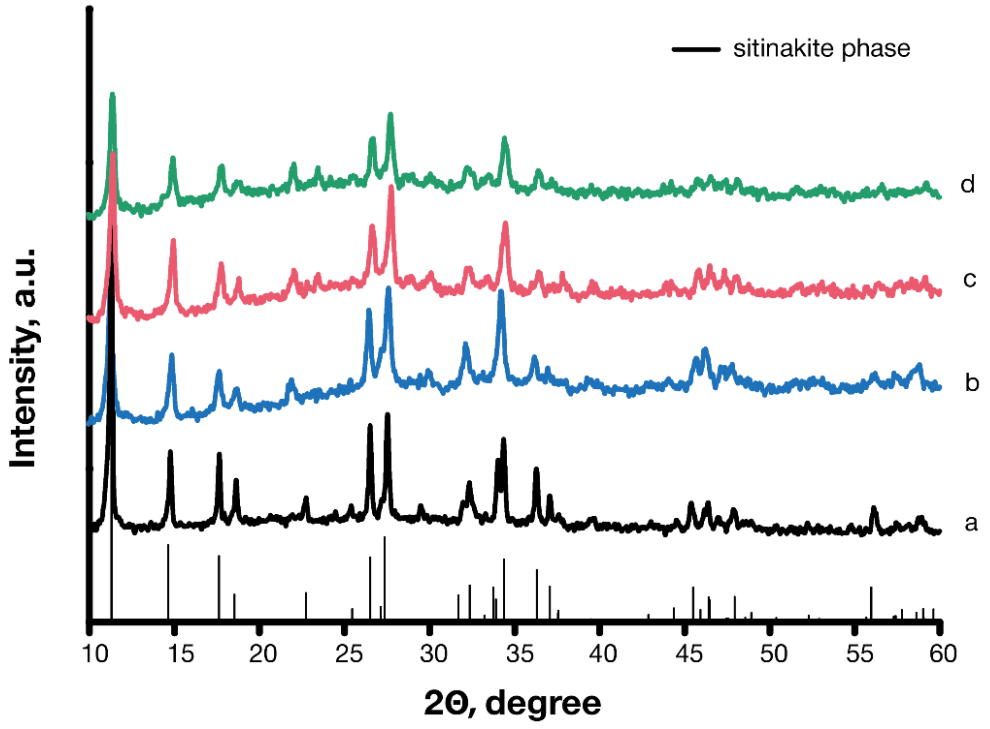

Figure S1. XRD patterns of: a – initial sample; b – treated with 0.01 M HCl; c – 0.1 M HCl; d – 1 M HCl.

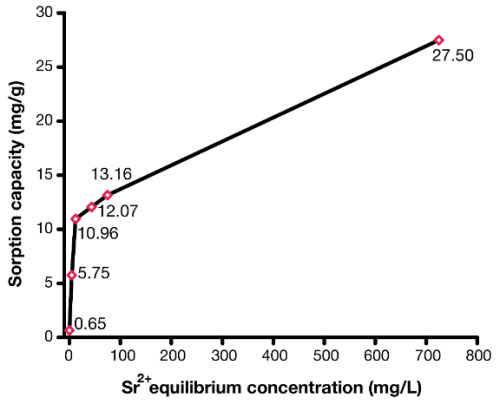

Figure S2. Isotherm of Sr^{2+} sorption by sitinakite at pH=6 (in the presence of NH_4OH).

Table S4. Sorption capacity of titanosilicate for the Sr^{2+} cation vs. temperature.
(pH is adjusted with NH_4OH, sample mass 0.02 g, solution volume 0.005 L, C_0 1000 mg/L)

pH	T, °C	C_p, mg/L	Sorption capacity		Amount of desorbed Na^+, meq/g
			mg/g	meq/g	
6.03 ± 0.10	20	890	27.50	0.64	2.24
	60	850	37.50	0.86	2.21
	100	823	44.27	1.00	2.19
8.05 ± 0.10	20	867	33.25	0.76	1.41
	60	792	52.00	1.18	1.89
	100	767	58.25	1.34	2.13

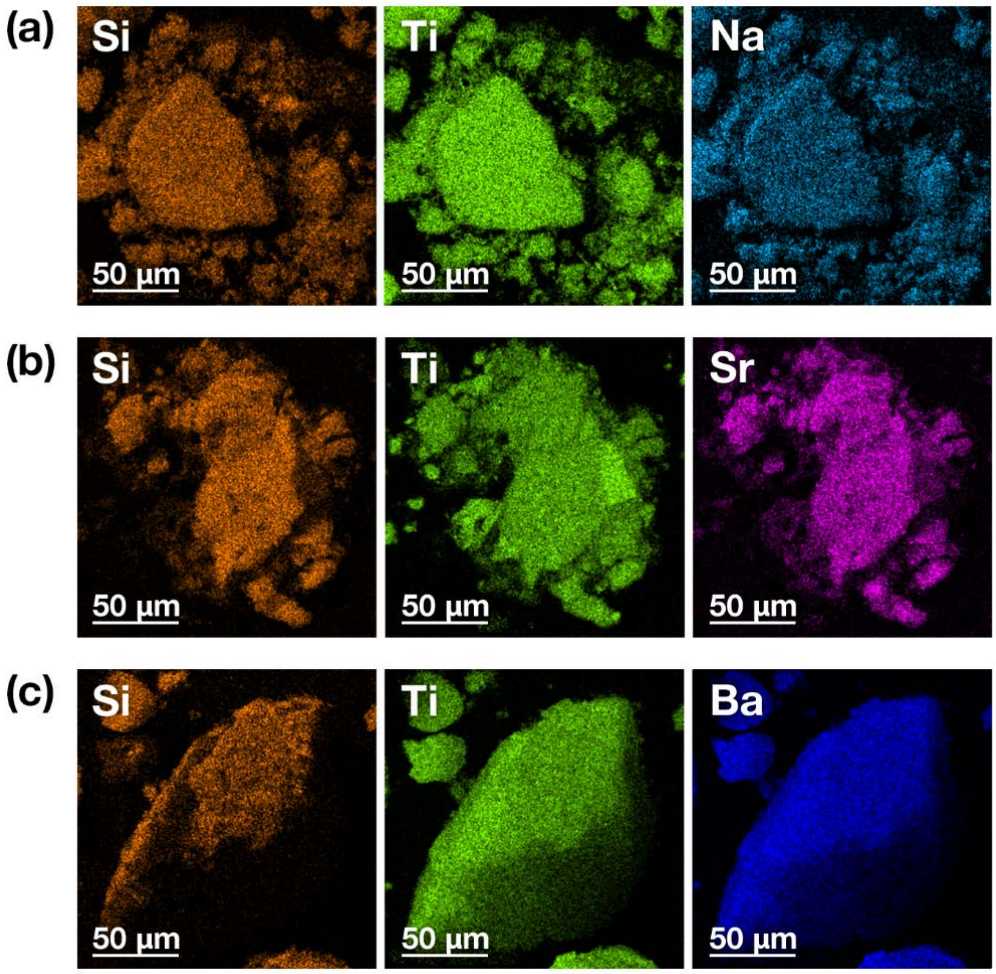

Figure S3. EDS mapping of sitinakite powder: a – initial sample; b – after adsorbing Sr^{2+} at 20°C; c – after adsorbing Ba^{2+} at 20°C.

Corresponding Author

*Elena F. Krivoshapkina: chemicalfox@mail.ru

*Igor A. Perovskiy: igor-perovskij@yandex.ru

Author Contributions

The manuscript was written through contributions of all authors. All authors have given approval to the final version of the manuscript. ‡These authors contributed equally.

Funding Sources

Russian Foundation for Basic Research, grant 16-35-00017 mol_a.

Ministry of Education and Science of Russian Federation, goszadanie no 11.1706.2017/4.6

ACKNOWLEDGMENT

Most of the characterization for the research materials was provided using the equipment of the Scientific Center Geonauka (Institute of Geology of Komi SC UB RAS). Perovskiy I.A. appreciates the financial support of the Russian Foundation for Basic Research [grant 16-35-00017 mol_a] and Program "Scientific basis for effective mining, the exploration and development of mineral resources base, development and implementation of innovative technologies, economic-geological zoning of Timan-Northern Ural region" [GR No. AAAA-A17-117121270037-4]. Pidko

E.A. and Khramenkova E. V are grateful to the Ministry of Education and Science of Russian Federation, goszadanie no 11.1706.2017/4.6.

REFERENCES

[1] W.J. Paulus, S. Komarneni,R. Roy, Bulk synthesis and selective exchange of strontium ions in Mica, *Nature*. 357 (1992) 571–573.

[2] F.P. Glasser, Progress in the immobilization of radioactive-wastes in cement, *Cem. Concr. Res.* 22 (1992) 201–209.

[3] S.N. Groudev, P.S. Georgiev,I.I. Spasova, K. Komnitsas, Bioremediation of a soil contaminated with radioactive elements, *Hydrometallurgy*. 59 (2001) 311–318.

[4] J.A. Entry, N.C. Vance, M.A. Hamilton, D.Zabowski, et al., Phytoremediation of soil contaminated with low concentrations of radionuclides, *Water Air Soil Pollut*. 88 (1996) 167–176.

[5] V. Luca, E. Drabarek, C. S. Griffith, The immobilization of cesium and strontium in ceramic materials derived from tungstate sorbents, *Scientific Basis for Nuclear Waste Management XXVII*. 807 (2004) 303–308.

[6] A. I. Ivanets, L. L. Katsoshvili, P. V. Krivoshapkin, et. al., Sorption of Strontium Ions onto Mesoporous Manganese Oxide of OMS-2 Type, *Radiochemistry*. 59 (2017) 264–271.

[7] B. Yildiz, H.N. Erten, M. Kis, The sorption behavior of Cs^+ ion on clay minerals and zeolite in radioactive waste management: sorption kinetics and thermodynamics, *J. Radioanal. Nucl. Chem*. 288 (2011) 275–283.

[8] A.M. El-Kamash, Evaluation of zeolite A for the sorptive removal of Cs^+ and Sr^{2+} ions from aqueous solutions using batch and fixed bed column operations, *J. Hazard. Mater*. 151 (2008) 432–445.

[9] O.B. Kotova, I.L. Shabalin, D.A. Shushkov, A.V. Ponaryadov, Sorbents based on mineral and industrial materials for radioactive wastes mmobilization, *Vestnik IG Komi SC UB RAS*. 2 (2015) 32–34.

[10] Y. Kakutani, P. Weerachawanasak, Y. Hirata, et.al., Highly effective K-Merlinoite adsorbent for removal of Cs^{+} and Sr^{2+} in aqueous solution, *The Royal Society of Chemistry Adv*. *7* (2017) 30919–30928.

[11] T. Moller, A. Clearfield, R. Harjula, Preparation of hydrous mixed metal oxides of Sb, Nb, Si, Ti and W with a pyrochlore structure and exchange of radioactive cesium and strontium ions into the materials, *Microporous Mesoporous Mater*. 54 (2002) 187–199.

[12] N.S. Rathore, A.P. Kumar, A.K. Venugopalan, Removal of actinides and fission products activity from intermediate alkaline wastes using inorganic exchangers, *J.Radioanal Nucl. Chem*. *262* (3) (2004), , 543–549.

[13] S.P. Mishra, D. Tiwari, S.K. Prasad, et.al., Inorganic ion exchangers in radioactive waste management part XVI: uptake of some metal phosphates (stannic and zirconium) for ^{134}Cs,*J Radioanal Nucl. Chem. 268* (2) (2006) 191–199.

[14] B. Yildiz, H.N. Erten, M. Kis, The sorption behavior of Cs^{+} ion on clay minerals and zeolite in radioactive waste management: sorption kinetics and thermodynamics, *J. Radioanal. Nucl. Chem.*288 (2011) 275–283.

[15] S. Duan, X. Xu, X.Liu, et. al., Highly enhanced adsorption performance of U(VI) by non-thermal plasma modified magnetic Fe_3O_4 nanoparticles, *J. of Colloid and Interface Science*. 513 (2018) 92–103.

[16] X. Liu, Y. Huang, S. Duan, Graphene oxides with different oxidation degrees for Co(II) ion pollution management, *Chemical Engineering Journal*. 302 (2016) 763–772.

[17] A. Anson, C.C.H. Lin, T.M. Kuznicki, et.al., Separation of ethylene/ethane mixtures by adsorption on small-pored titanosilicate molecular sieves, *Chemical engineering science*. 65(2012) 807–811.

[18] A. Clearfield, L.N. Bortun, A.I.Bortun, Alkali metal ion exchange by the framework titanium silicate $M_2Ti_2O_3SiO_4 \cdot nH_2O$ (M=H, Na), *Reactive & Functional Polymers.*43(2000) 85–95.

[19] J. Pérez-Carvajal, P. Lalueza, C. Casado, et. al. Layered titanosilicates JDF-L1 and AM-4 for biocide applications, *Applied Clay Science.* 56 (2012) 30–35.

[20] S.N. Britvin, L.G. Gerasimova, G.Yu. Ivanyuk, et. al., Application of titaniumcontaining sorbents for treating liquid radioactive waste with the subsequent conservation of radionuclides in Synroc titanate ceramics, *Theoretical Foundations of Chem. Eng*. 50 (4) 2016, 599–607.

[21] R.G. Anthony, C.V. Phillip, R.G. Dosch, Selective adsorption and ion exchange of metal cations and anions with silico-titanates and layered titanates, *Waste Manage*.13 (1993) 503–512.

[22] R.G. Anthony, R.G. Dosch, C.V. Phillip, Use of silicotitanates for removing cesium and strontium from defense waste, *Ind. Eng. Chem. Res.*33 (1994) 2702–2705.

[23] B.R. Cherry, M. Nyman, T.M. Alam, Investigation of cation environment and framework changes in silicotitanate exchange materials using solid-state ^{23}Na, ^{29}Si, and ^{133}Cs MAS NMR, *J. Solid State Chem.*177 (2004) 2079–2093.

[24] K.A. Venkatesan, V. Sukumaran, M.P. Antony, et. al., Studies on feasibility of using crystalline silicotitanates for the separation of cesium-137 from fast reactor high-level liquid waste, *J.Radioanal Nucl. Chem*. 280 (1) (2009) 129–136.

[25] S. Chitra, S. V. S. Viswanathan, P. K. Rao,et. al., Uptake of cesium and strontium by crystalline silicotitanates from radioactive wastes, *J Radioanal Nuc. Chem.*287 (2011) 955–960.

[26] T.J. Tranter, R.D. Tillotson, T.A. Todd, Evaluation of ionsiv™ IE-911 as a cesium removal option for ineel acidic tank waste, *Separ. Sci. Technol*. 40 (3) (2005) 157–170.

[27] T. Tomasberger, A.C. Veltkamp, A.S. Booij, et al., Radiocesium removal from high level liquid waste and immobilisation in sodium silicotitanate for geological disposa, *Radiochim. Acta*. 89 (3) (2001) 145–149.

[28] L. Al-Attar, A. Dyer, R. Harjula, Uptake of radionuclides on microporous and layered ion exchange materials, *J. Mater. Chem*. *13 (***2003)** 2963–2968.

[29] L. Al-Attar, A. Dyer, A. Pajanen, R. Harjula, Purification of nuclear wastes by novel inorganic ion exchangers, *J. Mater. Chem.* 13 (2003) 2969–2974.

[30] C. C. Pavel, M. Walter, P. Poml, Improvement of retention capacity of ETS-10 for uranyl ions by porosity modification and their immobilization into a titanosilicate matrix, *J. Mater. Chem*. 18 (2008) 3342–3346.

[31] A. E. Ringwood, S. E. Kesson, N. G. Ware, et al., Immobilisation of high level nuclear reactor wastes in SYNROC, *Nature*. 278 (1978) 219–223.

[32] A.E. Ringwood, S.E. Kesson, K.D. Reeve, *Radioactive waste forms for the future*. Lutze, W., Ewing, R.C.: Elsevier Science Publishers: North-Holland, Amsterdam, 1988, pp. 233–334.

[33] E. R. Vance, SYNROC – a suitable waste form for actinides, *MRS Bull*. 19 (12) (1994) 28–32.

[34] H. Xu, A. Navrotsky, M. D. Nyman, et al., Thermochemistry of microporous silicotitanate phases in the Na2O-Cs_2O-SiO_2- TiO_2-H_2O system, *J. Mater. Res*. 15 (2000) 815–823.

[35] H. Xu, A. Navrotsky, M. L. Balmer, et al., Energetics of substituted pollucites along the $CsAlSi_2O_6$-$CsTiSi_2O_{6,5}$ join: a hightemperature calorimetric strudy, *J. Am. Ceram. Soc*.84 (3) (2001) 555–560.

[36] Y. Su, M.L. Balmer, L. Wang, et al., Evaluation of thermally converted silicotitanate waste forms, *Materials Research Society Proc*. 556 (1999) 77–84.

[37] C.C. Pavel, M. Walter, P. Poml, et al., Contrasting immobilization behaviour of Cs^{+} and Sr^{2+} cations in a titanosilicate matrix, *J. Mater. Chem.*21 (2011) 3831–3837.

[38] D.M. Chapman, A.L. Roe, Synthesis, characterization and crystal chemistry of microporous titanium-silicate materials, *Zeolites.* 10 (1990) 730–741.

[39] W.T.A. Harrison, T.E. Gier, G.D. Stucky, Single-crystal structure of $Cs_3HTi_4O_4(SiO_4)_3{\cdot}4H_2O$, a titanosilicate pharmacosiderite analog, *Zeolites.*15(1995) 408-412.

[40] E.A. Behrens, D.M. Poojary, A. Clearfield, Syntheses, crystal structures, and ion-exchange properties of porous titanosilicates, $HM_3Ti_4O_4(SiO_4)_3{\cdot}4H_2O$ ($M = H^{+}$, K^{+}, Cs^{+}), structural analogues of the mineral pharmacosiderite, *Chem. Mater.* 8 (1996) 1236–1244.

[41] H.Xu, A. Navrotsky, M. Nyman, T. M. Nenoff, Crystal chemistry and energetics of pharmacosiderite-related microporous phases in the (K_2O)–(Cs_2O)–(SiO_2)–(TiO_2)–(H_2O) system, *Micropor. Mesopor. Mat.* 72 (2004) 209–218.

[42] V. Kostov-Kytin, R. Nikolova, N. Nakayama, et.al., New data on crystal chemistry of nano-sized microporous titanosilicates with pharmacosiderite structure, *Compt. rend. Acad. bulg. Sci.* 64 (5) (2011) 684-692.

[43] V.Kostov-Kytin, Hydrothermal synthesis of microporous titanosilicates, *Microporous and Mesoporous Materials.* 105 (2007) 32–238.

[44] D.G. Medvedev, A. Tripathi, A. Clearfield, et. al., Crystallization of Sodium Titanium Silicate with Sitinakite Topology: Evolution from the Sodium Nonatitanate Phase, *Chemistry of materials.* 16 (19) (2004) 3659-3666.

[45] V.Luca, Nb-substitution and Cs^+ ion-exchange in the titanosilicate sitinakite,*Micropor. and Mesopor. Mat.* 55 (2002) 1–13.

[46] D.Vuono, Synthesis and characterization of self-bonded ETS-4 and ETS-10 pellets, *Microporous and Mesoporous Materials.* 109 (2008) 118–137.

[47] N. Ismail, I. H. A. El-Maksod, H. Ezzat, Synthesis and characterization of titanosilicates rom white sand silica and its hydrogen uptake, *International journal of hydrogen energy.* 35 (2010) 10359–10365.

[48] L. Liua, R. Singh, G. Li, et. al., Synthesis and adsorption properties of titanosilicates ETS-4 and ETS-10 from fly ash, *J.of Hazard. Mater.*195 (2011) 340–345.

[49] Y.-C. Ng, C.-Y Jei, Shamsuddin, M. Titanosilicate ETS-10 derived from rice husk ash, *Microporous and Mesoporous Mater*. 122 (2009) 195–200.

[50] I.A. Perovskiy, G.V. Ignat'ev, *Ammonium fluoride method of desilication of leucoxene concentrate of Yarega deposit.* Predictive estimate of technological properties of minerals by applied mineralogy methods. Proc. of 7th Russian seminar of process mineralogy, Moscow, April, 9–11; Shchiptsov, V.V.; Karelian Scientific Centre RAS: Petrozavodsk, 2013, pp. 110–116.

[51] R.M. Aleksahin, N.P. Arhipov, R.M. Barhudarov, et al., Heavy natural radionuclides in the biosphere: Migration and biological effects on populations and ecosystems, Nauka Publ., Moscow, 1990.

[52] N.G. Rachkova, I.I. Shuktomova, The role of sorbents in processes of transformation of compounds of uranium, radium and thorium in podsolic soil, Nauka Publ., St.Petersburg, 2006.

[53] T.S. Dobrolyubskaya, Fluorescent Method, in Analiticheskayakhimiyaurana (Analytical Chemistry of Uranium), Nauka Publ., Moscow, 1962, pp. 143–165.

[54] V.I. Kuznetsov, V.B. Savvin, Delicate photometrical determination of thorium with reagent arsenazo III, *Radiochemistry*. 3 (1961) 79–86.

[55] J.P. Perdew, K. Burke, M. Ernzerhof, Generalized gradient approximation made simple, *Phys. Rev. Lett*.77 (1996) 3865–3868.

[56] G. Kresse, D. Joubert, From ultrasoft pseudopotentials to the projector augmented-wave method, *Phys. Rev. B.* 59 (3) (1999) 1758 –1775.

[57] P. E. Blöchl, Projector augmented-wave method, *Phys. Rev. B.* 50 (1994) 17953 –17 979.

[58] G. Kresse, J. Hafner, Ab initio molecular dynamics for open-shell transition metals, *Phys. Rev*. 48 (1993) 13115–13118.

[59] G. Kresse, J. Hafner, Ab-initio molecular-dynamics simulation of the liquid-metal–amorphous-semiconductor transition in germanium, *J. Phys. Rev*.49 (1994) 14251–14269.

[60] G. Kresse, J. Furthmuller, Efficiency of ab-initio total energy calculations for metals and semiconductors using a plane-wave basis set, *Comput. Mater. Sci*. 6 (1996) 15–50.

[61] G. Kresse, J. Furthmuller, Efficient iterative schemes for ab initio total-energy calculations using a plane-wave basis set, *J. Phys. Rev*.54 (1996) 11169–11186.

[62] H.X. Zhu,P.X. Zhou, X. Li, et.al.,Electronic structures and optical properties of rutile TiO_2 with different point defects from DFT +U calculations, *Phys. Letters A*. 378 (2014) 2719–2724.

[63] G. Beridze, P.M. Kowalski, Benchmarking the DFT+U Method for Thermochemical Calculations of Uranium Molecular Compounds and Solids, *J. Phys. Chem. A*. 118 (50) (2014) 11797–11810.

[64] H. J. Monkhorst, J.D. Pack, Special points for Brillouin-zone integrations, *Phys. Rev. B*. 13 (12) (1976) 5188 – 5192.

[65] E.V. Sokolova, R.K. Rastsvetaeva, V.I. Andrianov, et al., Crystal structure of a new natural sodium titanosilicate, *Reports of the USSR Academy of Sciences*. 307 (1989) 114–117.

[66] V.A. Kulagin, T.A. Kulagina, A.I. Matyushenko, Recycling of spent nuclear fuel and radioactive waste management, *Journal of Siberian Federal University. Engineering & Technologies*. 6 (2013) 123–149.

[67] A.I. Nikolaev, G. Yu, S.V. Ivanyuk, et al., Nanoporoustitanosilicates: crystal chemistry, localization conditions in alkaline massifs and prospects synthesis, *Herald of the Kola Science Centre RAS*. 4(2010) 51–62.

[68] A.I. Orlova, N.V. Malanina, V.N. Chuvil'Deev, et. al., Praseodymium and neodymium phosphates $Ca_9Ln(PO_4)_7$ of whitlockite structure: Preparation of a ceramic with a high relative density, *Radiochemistry*. 56 (4) (2014) 380–384.

[69] A.E. Ringwood, S.E. Kesson, K.D. Reeve, et al.,"Synroc" in Radioactive Waste for the Future. Elsevier: New York, 1988, pp. 233–334.

[70] Yu.P. Menshikov, E.V. Sokolova, et al.,Sitinakite $Na_2KTi_4Si_2O_{13}(OH)\cdot 4H_2O$ – a new mineral, *Proceedings of the Russian Mineralogical Society*. 121 (1992) 94–99.

[71] X. Xie, R. Deng, Y. Pang, et. al., Adsorption of copper(II) by sulfur microparticles, *Chemical Engineering Journal*. 314 (2017) 434–442.

[72] N.V. Chukanov, *Infrared spectra of mineral species. Springer Geochemistry*, Mineralogy, 2014.

[73] B.J. Aragão, Y. Messaddeq, Peak separation by derivative spectroscopy applied to ftir analysis of hydrolized silica, *J. Braz. Chem*. Soc. 19 (8) (2008) 1582–1594.

[74] I.I. Plyusnina, *Infrared spectra of minerals*, Metallurgiya Publ., Moscow, 1977.

[75] J. Madejova, P. Komadel, Baseline studies of the clay minerals society source clays: infrared methods,*Clays and Clay Minerals*. 49 (5) (2001) 410–432.

[76] A. Pirson, A. Mohsine, R. Marcot, et al., Synthesis of SiO_2-TiO_2Xerogels by Sol-Gel Process, *J. of Sol-Gel Science and Technology*. 4 (1995) 179–185.

[77] A. Chaisena, Synthesis of sodium zeolites from lampang diatomite applied for ammonium ion removal, Submitted of Philosophy in Chemistry, Thailand, 2004.

[78] F. Granados-Correa, J. Jiménez-Becerril, Chromium (VI) adsorption on boehmite,*J. Hazard. Mater.*162 (2009) 1178–1184.

[79] X.K. Wang, C.L. Chen, J.Z. Du, et.al., Effect of pH and aging time on the kinetic dissociation of ^{243}Am(III) from humic acid-coated c-Al_2O_3: a chelating resin exchange study, *Environ. Sci. Technol.* 39 (2005) 7084–7088.

[80] H.T. Xing, J.H. Chen, X. Sun, Y.H. Huang, Z.B. Su, S.R. Hu, NH_2-rich polymer/graphene oxide use as a novel adsorbent forremoval of Cu(II) fromaqueous solution, *Chem. Eng. J.* 263 (2015) 280–289.

[81] V. Neck, R. Müller, M. Bouby, M. Altmaier, et.al., Solubility of amorphous Th(IV) hydroxide – application of LIBD to determine the solubility product and EXAFS for aqueous speciation. *Radiochim. Acta*, 90 (2002) 485–494.

[82] M. Ochs, D. Mallants, L. Wang, Sorption Values for Thorium, Uranium, Plutonium, Neptunium, and Protactinium, *Radionuclide and Metal Sorption on Cement and Concrete*, 2015, pp. 121–170.